Quantum Interference Mapping of Rashba-Split Bloch States in Bi/Ag(111)

L. El-Kareh,[1] P. Sessi,[1,*] T. Bathon,[1] and M. Bode[1,2]

[1]*Physikalisches Institut, Experimentelle Physik II, Universität Würzburg, Am Hubland, D-97074 Würzburg, Germany*
[2]*Wilhelm Conrad Röntgen-Center for Complex Material Systems (RCCM), Universität Würzburg, Am Hubland, D-97074 Würzburg, Germany*

(Received 15 January 2013; revised manuscript received 28 February 2013; published 23 April 2013)

We report on low-temperature scanning tunneling spectroscopy investigations of the $(\sqrt{3}\times\sqrt{3})$ Bi/Ag(111)$R30°$ surface alloy which provides a giant Rashba-type spin splitting. We observed spectroscopic features that are assigned to two Rashba-split bands. Quantum interference mapping shows that backscattering is not only allowed below but also above the Rashba energy. We argue that the observed behavior can be understood within the Bloch picture where k refers to the crystal momentum and the velocity of an electronic state is defined as $v_n(E) = \frac{1}{\hbar}\nabla_k E_n(k)$. The analysis of the energy dispersion of scattering channels reveals a conventional Rashba splitting for the unoccupied Rashba bands, while hybridization is observed in the occupied states.

DOI: 10.1103/PhysRevLett.110.176803 PACS numbers: 73.20.At, 68.37.Ef, 71.70.Ej

It is well known that the degeneracy of electronic states can be lifted by breaking the inversion symmetry of crystal lattices intrinsically (Dresselhaus effect) [1] or by introducing surfaces or interfaces (Rashba-Bychkov effect) [2]. While originally observed at interfaces of semiconductor heterostructures, the Rashba-Bychkov effect of metallic surfaces consisting of high-Z elements has recently attracted considerable interest. While the first successful observation of a Rashba-split surface state was reported for Au(111) by La Shell *et al.* [3], lately giant splittings have been found for $(\sqrt{3}\times\sqrt{3})$ surface alloys of heavy post-transition metals with noble metal fcc(111) surfaces [4–11].

In particular, the electronic structure of the $(\sqrt{3}\times\sqrt{3})$ Bi/Ag(111)$R30°$ surface has been the subject of numerous investigations [12–15]. This surface alloy features two downwards dispersing (effective electron mass $m^* < 0$) surface states within the L-projected bulk band gap, an occupied sp_z-like band and a (mostly) unoccupied p_x, p_y-derived band [12]. For both surface states significant Rashba splittings have been reported. While general consensus on the dispersion of the electronic bands has been reached, their spin polarization is still under discussion. The conventional Rashba model would lead to the spin structure schematically sketched in Fig. 1(a). In contrast, density-functional theory (DFT) calculations have predicted a more complicated spin topology [12], indicating that the spin polarization of the upper (empty) Rashba bands changes sign at the band maximum [Fig. 1(b)]. Furthermore, it has been predicted [12] and experimentally verified [14] that the upper and the lower Rashba band avoid hybridization due to spin-orbit–induced interband spin mixing. DFT calculations have predicted that both bands switch polarization at this point [Fig. 1(b)]. As has been pointed out in Ref. [5], peaks are observed at the respective band onsets [Fig. 1(c)].

Recently, Hirayama *et al.* [16] investigated the spin polarization of the $(\sqrt{3}\times\sqrt{3})$ Bi/Ag(111)$R30°$ surface alloy experimentally by studying the energy dependence of standing electron wave patterns with scanning tunneling spectroscopy (STS). This so-called quantum interference mapping technique observes spatial oscillations of the energy-resolved density of states which originate from elastic scattering between two momentum eigenstates of the sample, $k_{i,f}$. The resulting oscillation exhibits a wave vector which corresponds to the scattering vector $q(E) = k_f(E) - k_i(E)$.

Since electronic states with opposite spin polarization are orthogonal and cannot interfere, quantum interference patterns can only be observed if the spin polarization of the involved states is nonorthogonal [17,18] [see illustration in Fig. 1(d)]. While we cannot draw any conclusion on whether or not spin-flip processes exist [19], the existence of an interference pattern clearly shows that the eigenstates of the involved electronic states are nonorthogonal. As indicated qualitatively by black arrows in Figs. 1(a) and 1(b), the two cases sketched above are expected to yield in different evolutions of the energy-dependent scattering vector which can be distinguished by their qualitatively different quantum interference patterns.

Indeed, Hirayama *et al.* [16] observed pronounced oscillations which clearly showed an energy dispersion for the upper (empty) Rashba bands between the Rashba energy E_{R_1} and E_F [16], thereby indicating a conventional Rashba splitting as shown in Fig. 1(a). In contrast, no quantum interferences were observed above the Rashba energy, i.e., between E_{R_1} and E_1 [16]. This observation was interpreted to be a direct consequence of the spin structure shown in Fig. 1(a), which—according to Ref. [16]—leads to forbidden backscattering between E_1 and the Rashba energy E_{R_1}.

Here we revisit the $(\sqrt{3}\times\sqrt{3})$ Bi/Ag(111)$R30°$ surface alloy in a quantum interference study performed by scanning tunneling spectroscopy. In contrast to Hirayama *et al.* [16] who deposited the Bi on a thin Ag film epitaxially

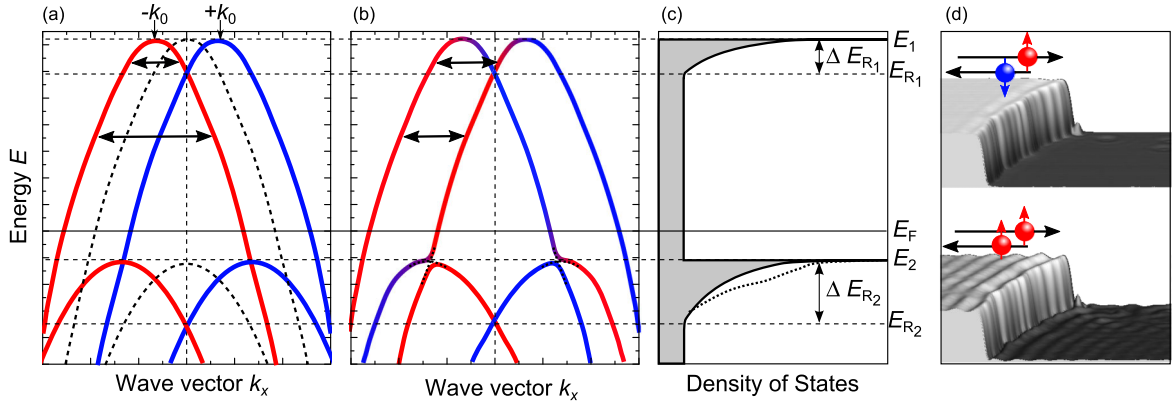

FIG. 1 (color online). Schematic representation of the $E(k_x)$ dispersion of Rashba-type spin-split bands and the resulting DOS in the case of two downwards dispersing surface states. Electrons in the red (blue) parabola exhibit spin polarization along $\pm\hat{y}$. (a) Within a conventional Rashba model the two parabolas are shifted along k_x by $\pm k_0$. (b) Density-functional theory (DFT) calculations have predicted a more complicated spin topology for the $(\sqrt{3}\times\sqrt{3})$ Bi/Ag(111)$R30°$ surface alloy [12]. (c) The theoretical DOS with singularities at the onset of the surface state bands. The opening of a hybridization gap leads to an enhanced DOS resulting in a shoulder at the asymmetric peak [hatched line]. (d) Illustration of the spin-dependence of quantum interference. Eigenstates of electrons with opposite spin polarization are orthogonal and cannot interfere (top). An interference pattern is expected for electrons with parallel spins (bottom).

grown on a Si(111) substrate, our study was performed on a Ag(111) single crystal. This minimizes the number of dislocations and is of particular advantage for the observation of short scattering vectors q which lead to relatively long-wavelength interference patterns in real space. For the upper Rashba band we observe quantum interferences below *and above* the Rashba energy E_{R_1}, indicating that backscattering is allowed within the Bloch picture. At energies corresponding to the position of the lower Rashba band the coexistence of two interference patterns with a large and a small scattering vector q is observed. The energy dispersion of these scattering vectors is explained by spin-orbit-induced spin mixing which leads to the opening of a hybridization gap and changes the spin polarization of the involved bands.

The experiments have been performed in a two-chamber UHV system equipped with a low-temperature STM working at 5 K. The system consists of separate chambers for sample preparation and surface analysis (base pressure $p \leq 1\times10^{-10}$ mbar). The Ag(111) single-crystalline substrate was cleaned by cycles of Ar^+ sputtering ($E =$ 500 eV) and subsequent annealing ($T \approx 700$ K). For preparation of the $(\sqrt{3}\times\sqrt{3})$ Bi/Ag(111)$R30°$ surface alloy a third of a Bi monolayer was evaporated onto the Ag(111) substrate held at $T \approx 470$ K. STS and dI/dU maps have been performed by means of standard lock-in technique ($\nu = 1.333$ kHz).

Figure 2 shows an averaged STS spectrum of the $(\sqrt{3}\times\sqrt{3})$ Bi/Ag(111)$R30°$ surface alloy. We can recognize two asymmetric peaks, that can clearly be assigned to the sp_z- derived (left side, occupied states) and the p_x, p_y-derived (right side, empty states) Rashba states [12,14]. We would like to emphasize that the edge singularity caused by the empty Rashba band appears about one order of magnitude more intense than in a previous publication [16]. The shape of both peaks closely resembles the singularities described in Ref. [6]. At the moment we can only speculate that the different measurement temperature (5 K vs 77 K), a lower modulation amplitude, and/or the better surface quality might lead to this improvement. Following the procedures given in Ref. [6] the peaks in the dI/dU spectrum were fitted by the blue lines in Fig. 2. Agreement with the experimental data is particularly good for the upper (empty) band for which we obtain $E_1 = 725$ meV and $\Delta E_{R_1} = 150$ meV. The overall agreement is also reasonable for the lower (occupied) Rashba band. Here the fit

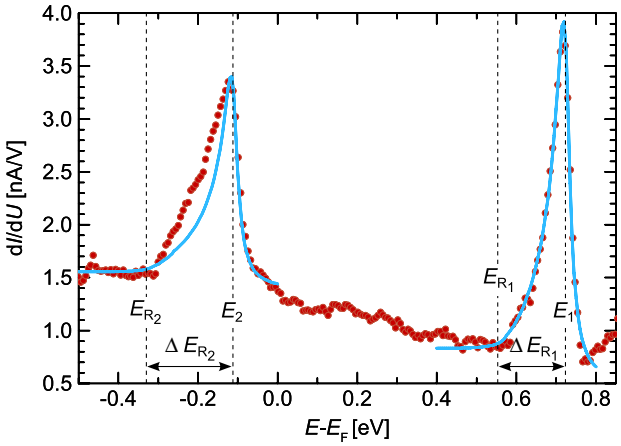

FIG. 2 (color online). Tunneling spectrum (red dots) of the $(\sqrt{3}\times\sqrt{3})$ Bi/Ag(111)$R30°$ surface alloy showing peaks at $E_1 = 725$ meV and $E_2 = -110$ meV (set point: $I_{set} = 1$ nA). The blue lines represent fits to the peaks (see text for details).

results in $E_2 = -110$ meV and $\Delta E_{R_2} = 220$ meV, which is consistent with earlier angular-resolved photoemission spectroscopy (ARPES) and STS data [6].

However, the fitting procedure cannot reproduce the shoulder which appears at the left flank of the peak. We believe that this shoulder is the spectroscopic evidence for the gap opening at the hybridization point of the two Rashba bands which occurs at an energy of about 200 meV below E_F (see Fig. 1). Without spin-orbit coupling the pure spin states of both bands were orthogonal and the bands could cross. Since the spin-orbit coupling in the Bi/Ag alloy is indeed strong, considerable spin-mixing occurs, resulting in the opening of a hybridization gap [12,14]. This leads to a reduced band velocity and thereby enhances the DOS [20].

To obtain the energy dispersion we measured a series of dI/dU maps in the bias range between -400 meV up to $+800$ meV (increment 50 meV). Figure 3(a) shows the topography of the investigated sample area. We can recognize atomically flat terraces which are separated by three step edges with different crystallographic directions. The inset shows an atomically resolved image of the Bi alloy. Arrows show crystallographic directions relative to the Bi overlayer, which is rotated by 30° with respect to the Ag(111) substrate, i.e., $\overline{\Gamma K}_{\mathrm{Bi}} \parallel \overline{\Gamma M}_{\mathrm{Ag}}$ and $\overline{\Gamma M}_{\mathrm{Bi}} \parallel \overline{\Gamma K}_{\mathrm{Ag}}$.

Figures 3(b) and 3(c) show the interference patterns measured at $U = +137$ meV and $U = +587$ meV, i.e., below and above the Rashba energy E_{R_1} of the upper Rashba band, respectively. Although the pattern above E_{R_1} is far less structured than the one below in both cases standing waves parallel to step edges are clearly visible [21]. This observation is in contrast to Ref. [16], where the absence of an interference pattern above E_{R_1} was interpreted in terms of forbidden backscattering of a Rashba-split surface state. We have analyzed our data quantitatively by two-dimensional Fourier transformation (2D-FFT). Figure 3(d) shows the 2D-FFT of the data presented in (b). One can recognize straight lines which fan out from the center and a

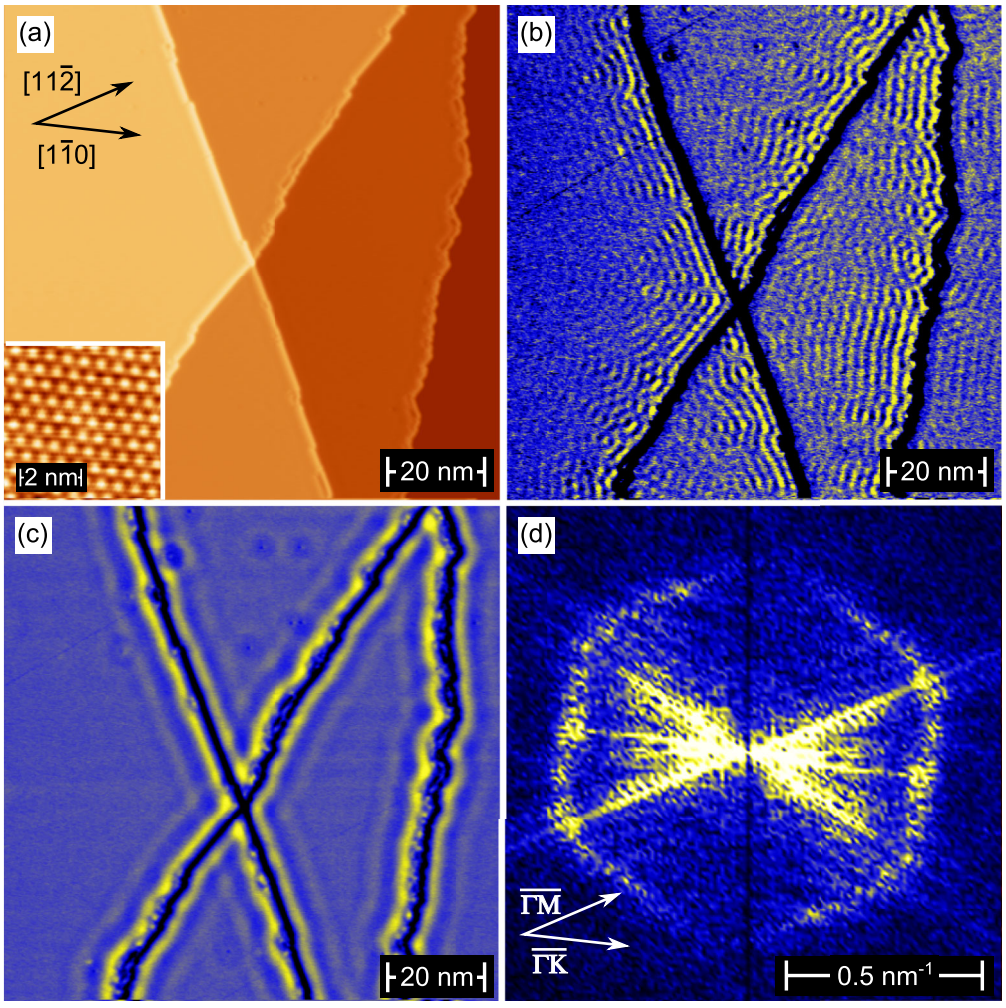

FIG. 3 (color online). (a) Constant-current image of the $(\sqrt{3} \times \sqrt{3})$ Bi/Ag(111)$R30°$ surface alloy. Inset: Atomic scale image. (b) dI/dU map measured at $U = 137$ meV and (c) at $U = 587$ meV. (d) Corresponding two-dimensional Fourier transform of (b). The hexagonal shape depicts an anisotropic dispersion for $\overline{\Gamma K}$ and $\overline{\Gamma M}$ directions.

hexagonally shaped frame with intensity maxima at the edges and at the middle of the side, i.e., along the $\overline{\Gamma M}$ and the $\overline{\Gamma K}$ direction, respectively. The fanning-out lines, which are rotated by $\frac{\pi}{2}$ relative to the real space image due to the FFT processing, originate from the step edges. Correspondingly, the maxima at the edges and sides of the hexagon on the 2D-FFT are caused by the quantum interference pattern formed by the scattering vector q which connects two nonorthogonal electron eigenstates.

The extracted $q(E)$ values are displayed in Fig. 4. Clearly, we observe an energy dispersion for both Rashba bands. Scattering within the p_x, p_y-derived band (labeled D_1 in Fig. 4) starts at about +700 meV. In the energy range between the Rashba energy E_{R_1} of the p_x, p_y-derived band and E_F our data are fully consistent with the data presented in Ref. [16], thereby confirming a conventional Rashba state in this energy range. Indeed, our data clearly show the existence of an interference pattern and a dispersion of the scattering vector even above the Rashba energy E_{R_1}, i.e., within the energy range where—according to Ref. [16]—backscattering is forbidden.

At this point it is important to note that the involved electrons occupy Bloch states. Therefore, k refers to the crystal momentum rather than the electron momentum and k itself is no longer suitable to determine if backscattering is allowed. Instead, the band velocity for Bloch states is defined as $v_n(E) = \frac{1}{\hbar}\nabla_k E_n(k)$ and one would expect that spin-conserved backscattering can occur between sections with positive and negative slope ∇_k, i.e., positive and negative band velocity. In contrast to the observations reported in Ref. [16] this is indeed possible below and above the Rashba energy.

Fitting our data to a parabolic dispersion yields $E_1 = (737 \pm 20)$ meV for the p_x, p_y-derived state. This value is in agreement with our STS data presented in Fig. 2. For the effective mass we obtain $m^*_{\overline{\Gamma M}} = (-0.40 \pm 0.09)m_e$ and $m^*_{\overline{\Gamma K}} = (-0.34 \pm 0.08)m_e$.

Because of the hybridization between sp_z- and p_x, p_y-derived states, the interpretation of the interference patterns observed for energies below −100 meV is more complex. For some energies we even observe the coexistence of two interferences, indicating the presence of two different spin-conserving scattering channels (see D_2 and D_3 at energies $E - E_F < -100$ meV in Fig. 4). Fitting the inner dispersion D_2 by a parabola would lead to $m^*_{\overline{\Gamma K}} = (-0.09 \pm 0.01)m_e$ and $m^*_{\overline{\Gamma M}} = (-0.13 \pm 0.02)m_e$ which is far below values determined by ARPES measurements ($m^* = -0.35m_e$) [5,9].

Instead, as schematically shown in Fig. 5, we assign our data to scattering vectors between the two Rashba bands which change spin polarization as they hybridize. This result is qualitatively consistent with earlier DFT calculations [12]. Following the representation chosen in a spin-ARPES experiment performed by Meier *et al.* [13], the inner branches of the contributing p_x, p_y- and sp_z-derived branches were labeled l_1 through r_3 (see bottom of Fig. 5). Rather than scattering between branches l_3 and r_1 or l_1 and r_3, the inverted polarization now allows for scattering between l_2 and r_1 (upper black arrow in Fig. 5) or l_3 and r_2 (lower arrow), which exhibit the same spin polarization.

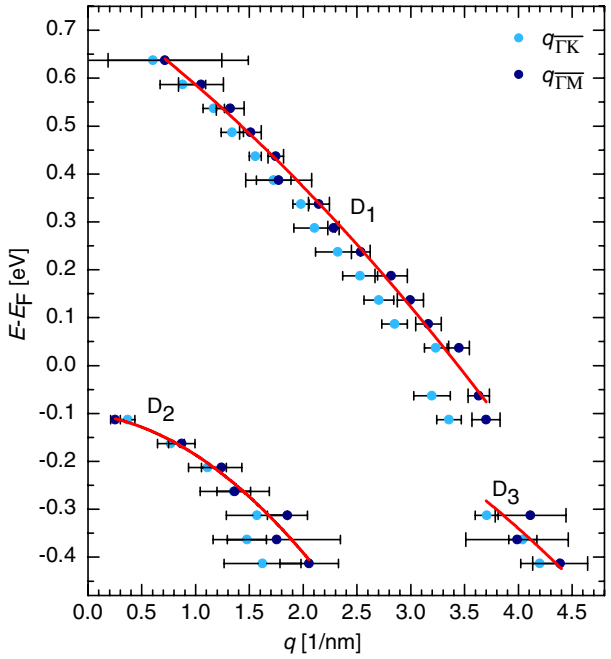

FIG. 4 (color online). Dispersion of scattering vector q as extracted from a series of dI/dU maps. Data measured along the $\overline{\Gamma K}$ and $\overline{\Gamma M}$ directions are plotted in light blue and dark blue color, respectively. Red lines are guides for the eye only.

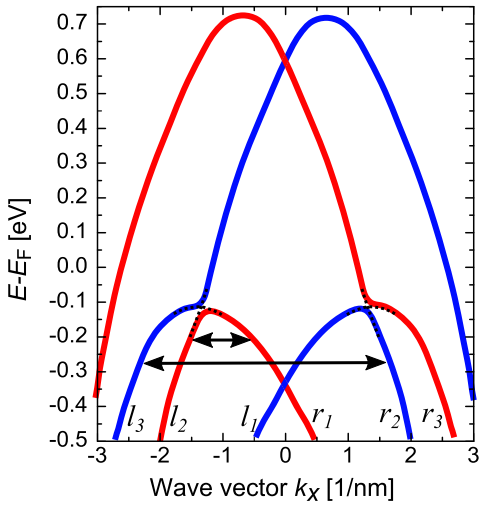

FIG. 5 (color online). Proposed spin topology of the $(\sqrt{3} \times \sqrt{3})$ Bi/Ag(111)$R30°$ surface alloy. Above the Fermi level E_F the upper band exhibits a conventional Rashba splitting. The spin topology of the lower band is more complicated as it hybridizes with the inner branch of the upper Rashba band. Arrows indicate the two scattering channels observed in the occupied states.

Indeed, the spin-ARPES experiments show that the respective branches are essentially polarized along the y axis (see Table I in Ref. [13]). As a result the scattering vector between l_2 and r_1 becomes very short and the resulting dispersion suggests an effective electron mass which is no longer representative for electrons in the sp_z-derived bands. Correspondingly, we can assign the larger scattering vector to an interference between the branches l_1 and r_2 (lower black arrow in Fig. 5) or l_2 and r_3. Although spin- and angle-resolved photoemission spectroscopy experiments have shown a considerable out-of-plane component for sp_z–derived branches l_1 and r_3, the in-plane component of these branches is essentially aligned with those of r_2 and l_2 [13], respectively, thereby enabling scattering and a relative high intensity in the quantum interference pattern. We speculate that the change of spin orientation occurs around the hybridization energy, as this is where the scattering vectors associated with a conventional Rashba bands (labeled D_1 in Fig. 4) are vanishing and scattering vectors D_3 are appearing.

In summary we have revisited the quantum interference patterns formed by Rashba-split surface states in $(\sqrt{3} \times \sqrt{3})$ Bi/Ag(111)$R30°$ surface alloy. For the empty states the observed energy dispersion between the Rashba energy and the Fermi level is in agreement with an earlier study [16] and confirms conventional Rashba behavior. In addition we also observe quantum interferences above the Rashba energy indicating that backscattering is allowed within the Bloch picture. Careful analysis of scattering patterns below the Fermi level reveals the coexistence of two scattering vectors. The energy dispersion is explained by the opening of a hybridization gap due to spin-orbit–induced spin mixing.

This work has been funded by Grant No. BO1468-20 (FOR1162). We acknowledge valuable discussions with C. R. Ast and H. Bentmann.

*Corresponding author.
sessi@physik.uni-wuerzburg.de

[1] G. Dresselhaus, Phys. Rev. **100**, 580 (1955).
[2] Y. A. Bychkov and E. I. Rashba, J. Phys. C **17**, 6039 (1984).
[3] S. LaShell, B. A. McDougall, and E. Jensen, Phys. Rev. Lett. **77**, 3419 (1996).
[4] D. Pacilé, C. R. Ast, M. Papagno, C. Da Silva, L. Moreschini, M. Falub, A. P. Seitsonen, and M. Grioni, Phys. Rev. B **73**, 245429 (2006).
[5] C. R. Ast, J. Henk, A. Ernst, L. Moreschini, M. C. Falub, D. Pacilé, P. Bruno, K. Kern, and M. Grioni, Phys. Rev. Lett. **98**, 186807 (2007).
[6] C. R. Ast, G. Wittich, P. Wahl, R. Vogelgesang, D. Pacilé, M. C. Falub, L. Moreschini, M. Papagno, M. Grioni, and K. Kern, Phys. Rev. B **75**, 201401 (2007).
[7] L. Moreschini *et al.*, Phys. Rev. B **79**, 075424 (2009).
[8] L. Moreschini, A. Bendounan, H. Bentmann, M. Assig, K. Kern, F. Reinert, J. Henk, C. R. Ast, and M. Grioni, Phys. Rev. B **80**, 035438 (2009).
[9] H. Bentmann, F. Forster, G. Bihlmayer, E. V. Chulkov, L. Moreschini, M. Grioni, and F. Reinert, Europhys. Lett. **87**, 37 003 (2009).
[10] H. Mirhosseini, J. Henk, A. Ernst, S. Ostanin, C.-T. Chiang, P. Yu, A. Winkelmann, and J. Kirschner, Phys. Rev. B **79**, 245428 (2009).
[11] J. Premper, M. Trautmann, J. Henk, and P. Bruno, Phys. Rev. B **76**, 073310 (2007).
[12] G. Bihlmayer, S. Blügel, and E. V. Chulkov, Phys. Rev. B **75**, 195414 (2007).
[13] F. Meier, H. Dil, J. Lobo-Checa, L. Patthey, and J. Osterwalder, Phys. Rev. B **77**, 165431 (2008).
[14] H. Bentmann, S. Abdelouahed, M. Mulazzi, J. Henk, and F. Reinert, Phys. Rev. Lett. **108**, 196801 (2012).
[15] I. Gierz, F. Meier, J. H. Dil, K. Kern, and C. R. Ast, Phys. Rev. B **83**, 195122 (2011).
[16] H. Hirayama, Y. Aoki, and C. Kato, Phys. Rev. Lett. **107**, 027204 (2011).
[17] J. I. Pascual *et al.*, Phys. Rev. Lett. **93**, 196802 (2004).
[18] P. Roushan, J. Seo, C. V. Parker, Y. S. Hor, D. Hsieh, D. Qian, A. Richardella, M. Z. Hasan, R. J. Cava, and A. Yazdani, Nature (London) **460**, 1106 (2009).
[19] L. Petersen and P. Hedegård, Surf. Sci. **459**, 49 (2000).
[20] M. Bode, S. Heinze, A. Kubetzka, O. Pietzsch, X. Nie, G. Bihlmayer, S. Blügel, and R. Wiesendanger, Phys. Rev. Lett. **89**, 237205 (2002).
[21] We believe that the much weaker interference pattern above E_R is caused by a strong reduction of lifetime/coherence length of states far above E_F. It is well known that electronic states close to the Fermi level exhibit a relatively long lifetime leading to a more pronounced interference pattern and that the lifetime progressively decreases as the energetic distance to the Fermi level (excess energy) is increased [22].
[22] L. Bürgi, O. Jeandupeux, H. Brune, and K. Kern, Phys. Rev. Lett. **82**, 4516 (1999).